X-ray Crystallographic Analysis of Inhibition of Endothiapepsin by Cyclohexyl Renin Inhibitors†,‡

J. Cooper,* W. Quail,§ C. Frazao,‖ S. I. Foundling,⊥ and T. L. Blundell

Laboratory of Molecular Biology, Department of Crystallography, Birkbeck College, Malet Street, London WC1E 7HX, U.K.

C. Humblet and E. A. Lunney

Parke-Davis Pharmaceutical Research Division, Warner-Lambert Company, 2800 Plymouth Road, Ann Arbor, Michigan 48105-2430

W. T. Lowther and B. M. Dunn

Department of Biochemistry and Molecular Biology, University of Florida College of Medicine, Box-100245, Health Science Center, Gainesville, Florida 32610-0245

Received January 22, 1992; Revised Manuscript Received May 20, 1992

ABSTRACT: The crystal structures of endothiapepsin, a fungal aspartic proteinase (EC 3.4.23.6), cocrystallized with two oligopeptide renin inhibitors, PD125967 and PD125754, have been determined at 2.0-Å resolution and refined to *R*-factors of 0.143 and 0.153, respectively. These inhibitors, which are of the hydroxyethylene and statine types, respectively, possess a cyclohexylalanine side chain at P_1 and have interesting functionalities at the P_3 position which, until now, have not been subjected to crystallographic analysis. PD125967 has a bis(1-naphthylmethyl)acetyl residue at P_3, and PD125754 possesses a hydroxyethylene analogue of the P_3–P_2 peptide bond for proteolytic stability. The structures reveal that the S_3 pocket accommodates one naphthyl ring with conformational changes of the Asp 77 and Asp 114 side chains, the other naphthyl group residing in the S_4 region. The P_3–P_2 hydroxyethylene analogue of PD125754 forms a hydrogen bond with the NH of Thr 219, thereby making the same interaction with the enzyme as the equivalent peptide groups of all inhibitors studied so far. The absence of side chains at the P_2 and P_1' positions of this inhibitor allows water molecules to occupy the respective pockets in the complex. The relative potencies of PD125967 and PD125754 for endothiapepsin are consistent with the changes in solvent-accessible area which take place on inhibitor binding.

The aspartic proteinases are a homologous group of enzymes involved in extra- and intracellular digestion. One member of this family is renin which catalyzes the initial step of the renin–angiotensin cascade leading to formation of a potently vasoactive peptide: angiotensin II. Renin inhibitors have been shown to lower blood pressure in vivo albeit with short duration [e.g., Leckie (1985)]. Most inhibitors have been developed from the minimal substrate sequence which consists of residues 6–13 of the natural substrate angiotensinogen. Replacement of the scissile Leu–Val bond with various nonhydrolyzable analogues has given compounds with potencies better than 10^{-9} M [for reviews, see Blundell et al. (1987) and Cooper and Harris (1988)]. In general, the closer the analogue to the putative intermediate of hydrolysis [$-C(OH)_2NH_2^+-$] the greater its potency.

Statine analogues, which are derived from a naturally occurring aspartic proteinase inhibitor mimicking one hydroxyl of the putative intermediate, are of the general form C_α–CHOH–CH_2–CO–NH–C_α. Cocrystallization of a statyl inhibitor with endothiapepsin has shown that the statine residue occupies both S_1 and S_1' subsites, thereby mimicking a dipeptide analogue (Cooper et al., 1989). In contrast, hydroxyethylene analogues which are of the form C_α–CHOH–CH_2–C_α do not introduce such a frame shift. Inhibitors containing these analogues have been developed to achieve potencies for human renin in the nanomolar range (Szelke et al., 1982; Szelke, 1985).

Analogues designed to mimic the scissile –Leu–Val– peptide bond of human renin can be improved significantly by use of cyclohexylmethyl for the P_1 side chain. This has been shown to increase the potency by 2 orders of magnitude relative to the equivalent isobutyl (leucine-like) analogue (Boger et al., 1985). For most inhibitors cyclohexylmethyl is optimal for the S_1 pocket of renin. As can be seen in Figure 1, both inhibitors used in this study have a cyclohexylmethyl group at P_1 and contain hydroxyethylene and statine transition-state analogues.

Several compounds have been reported which possess naphthylalanine or bis(1-naphthylmethyl)acetyl at P_3 (Iizuka et al., 1988; Kokubu et al., 1985; 1986; Luly et al., 1987). Compounds of this type, e.g., PD125967 (Figure 1), have IC_{50}'s for renin in the nanomolar range. It was therefore of considerable interest to us to discover how such bulky aromatic groups are accommodated by the substrate binding cleft of an aspartic proteinase.

The S_2 subsite of aspartic proteinases appears to be one of the least specific; the bound X-ray structures of renin inhibitors

† We acknowledge the financial support of the Science and Engineering Research Council, the Agricultural and Food Research Council, the Medical Research Council (U.K.), and the NIH (DK 18865).

‡ Crystallographic coordinates have been deposited in the Brookhaven Protein Data Bank under the code 4ER1.

* To whom correspondence should be addressed.

§ On sabbatical leave from the Department of Chemistry, University of Saskatoon, Saskatoon, Canada.

‖ Present address: Centro do Technologia Quimica & Biologica, Lisbon, Portugal.

⊥ Present address: Oklahoma Medical Research Foundation, University of Oklahoma Health Science Center, Oklahoma City, OK.

0006-2960/92/0431-8142$03.00/0

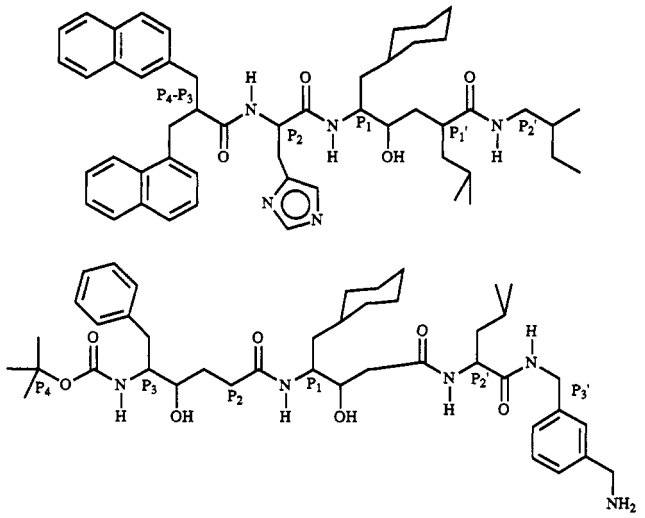

FIGURE 1: Chemical structures of PD125967 (top) and PD125754 (bottom).

complexed with endothiapepsin have shown that His at P_2 can adopt different χ_1 angles separated by up to 120° [e.g., Šali et al. (1989)]. The degree of exposure to solvent suggests that the potency may be retained in the absence of a side chain at this position, thereby lowering the molecular weight of the inhibitor. Accordingly, the inhibitor PD125754 (Figure 1) was synthesized with the equivalent of a glycine residue at P_2.

Peptides, when administered orally, are susceptible to degradation in the stomach by gastric enzymes and the proteinases of the pancreas and brush border of the small intestine. Their lifetimes in the plasma are often short due to rapid proteolysis and other metabolic processes. The P_3 Phe–P_2 His bond of a renin inhibitor was demonstrated to be cleaved by chymotropsin (Rosenberg et al., 1987) in accordance with the known specificity of this enzyme. The replacement of Phe at P_3 with *O*-methyl-Tyr was shown to abolish chymotrypsin cleavage and yet retain high inhibitory potency for renin (Bolis et al., 1987). Hydrolysis by chymotrypsin is also abolished by use of a naphthyl residue at P_3 (Kissei, 1988) as is likely to be the case for PD125967 (Figure 1). Hydrolysis is also abolished by replacement of the P_3–P_2 peptide bond with various nonhydrolyzable analogues; for example, PD125754 possesses a hydroxyethylene (–CHOH–CH_2–) replacement here (Figure 1).

In this paper we report the structures of both PD125967 and PD125754 complexed with endothiapepsin and refined at 2.0-Å resolution against X-ray data collected by a FAST area detector. The cocrystals were not isomorphous with native endothiapepsin but grew with the same unit cell as another complex (BW625) previously solved by molecular replacement (Cooper, 1989). The structures were solved by the difference Fourier method and least-squares refinement. The resulting electron density maps defined the inhibitor conformations clearly and showed that one of the bis(1-naphthylmethyl) groups at P_3 of PD125967 is accommodated by significant conformational changes of side chains at positions 77 and 114. The P_3–P_2 hydroxyethylene analogue of PD125754 retains the hydrogen bond with Thr 219 observed in complexes of other inhibitors which possess a peptide group at this position [e.g., Foundling et al. (1987)].

METHODS

Synthesis of Inhibitors and Biological Activity. Syntheses of PD125967 and PD125754 and measurements of their affinity for renin have been described elsewhere (Kaltenbronn et al., 1990a,b; Hudspeth et al., 1989). Measurements of the K_i values for endothiapepsin were made by use of a chromogenic octapeptide, P-P-T-I-F-NPh-R-L (where NPh = *p*-nitrophenylalanine). The hydrolysis of this substrate was measured from the average decrease in absorbance from 284 to 324 nm using a Hewlett-Packard 8452A diode array spectrophotometer (Dunn et al., 1986). Inhibitors were dissolved initially in DMSO, and all reactions were performed at 37 °C in 0.1 M sodium formate, pH 3.5, and 4% DMSO. Following preincubation of the enzyme at 37 °C for 3 min, the initial rates of six different substrate concentrations around K_m ($0.8K_m$ – $10K_m$) were measured. After preincubation with two or more inhibitor concentrations, additional curves were obtained from the initial rates from at least three different substrate concentrations. The K_i value from the family of curves was determined by Marquardt analysis and the equation $v = V_{max}[S]/[K_m(1 + [I]/K_i) + [S]]$.

Crystallization. The inhibitor cocrystals were grown by the same method as for native endothiapepsin (Moews & Bunn, 1970). A 10-fold molar excess of inhibitor was dissolved with freeze-dried enzyme and stirred for several hours. The solutions were centrifuged at 11000*g* to sediment insoluble material prior to addition of sufficient ammonium sulfate to achieve slight turbidity. The solutions were Millipore filtered, and saturated ammonium sulfate was added dropwise to achieve slight cloudiness which was then cleared by dropwise addition of acetone. The crystals grew after about 9 months.

Table I: X-ray Data for Inhibitor Cocrystals

	native	PD125967	PD125754
space group	$P2_1$[a]		
cell constants			
a (Å)	53.6	43.1	43.1
b (Å)	74.1	75.8	75.7
c (Å)	45.7	43.0	42.9
β (deg)	110.0	97.0	96.9
FAST data processing			
total no. of measured reflections		61099	88024
no. of unique reflections		17804	18024
merging *R*-factor[b] (intensities) (%)		6.1	9.5
completeness of data to 2.0 Å (%)		98	99

[a] International Tables, No. 4. [b] $R_{merge} = \sum_h\sum_i|I_{hi} - \langle I_h\rangle|/\sum_h N_h\langle I_h\rangle$, where h = reflection number, i = observation number, and N_h = number of observations of reflection h.

Table II: Refinement Statistics for the Inhibitor Complexes

	inhibitor	
	PD125967	PD125754
rms deviation from target bond lengths (Å)	0.025	0.024
rms deviation from target angle distances (Å)	0.050	0.029
rms deviation within nonbonded contact distances (Å)	0.063	0.034
rms distance from least-squares main-chain planes (Å)	0.018	0.010
rms deviation from least-squares side-chain planes (Å)	0.012	0.008
resolution range (Å)	20.0–2.0	20.0–2.0
R-factor	0.143	0.152
no. of cycles	73	34
mean U_{iso}'s[a] for		
enzyme (Å)	0.109 (2389)	0.131 (2389)
inhibitor (Å)	0.432 (60)	0.352 (45)
waters (Å)	0.367 (260)	0.382 (278)

[a] Number of atoms is shown in parentheses.

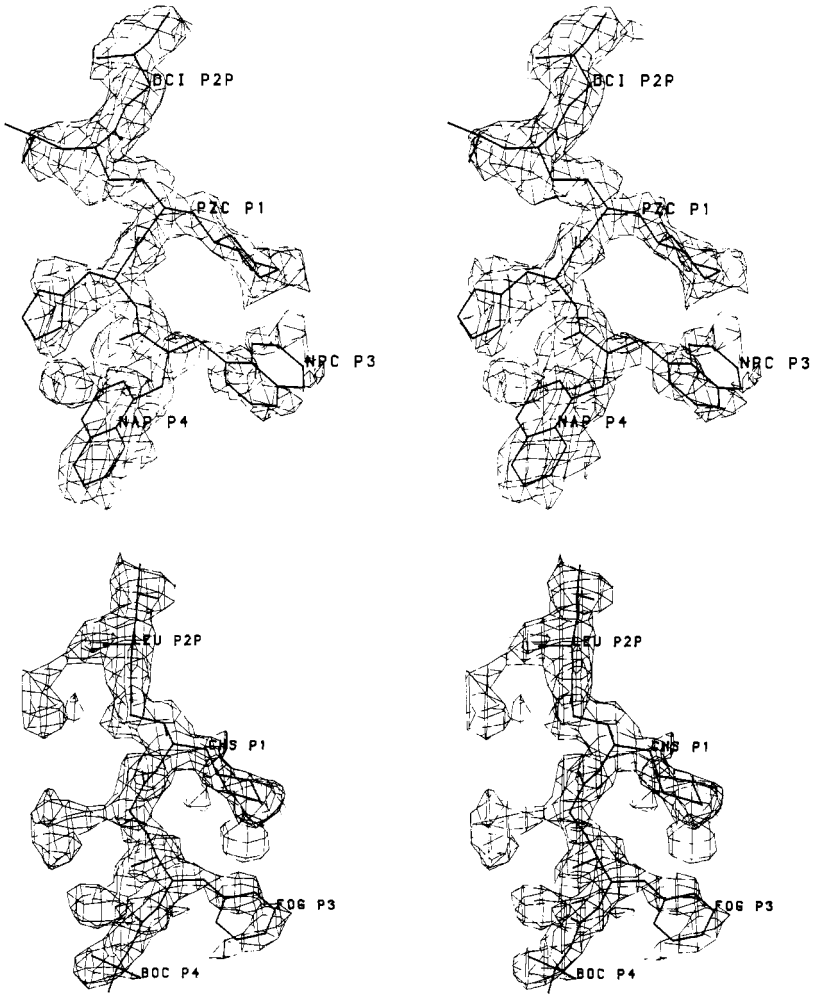

FIGURE 2: Initial difference Fouriers for PD125967 (top) and PD125754 (bottom) at 2.0-Å resolution calculated using Sim weights (Read, 1986). The inhibitors extend from P_4 to P_2' in the vertical direction. Electron density is shown in thin lines; inhibitors are shown as thick lines. The extra density at P_2 of PD125754 was interpreted as a water molecule (see Figure 3). P2P indicates the P_2' position.

The crystal shape was characteristic of previous nonisomorphous inhibitor complexes which have the same space group as the native enzyme ($P2_1$) but with a 20% lower unit cell volume (Table I). This results in much stronger diffraction intensity and greater longevity of the crystals, as well as giving a 20% reduction in the number of reflections which have to be measured to achieve a given resolution.

X-ray Analysis. X-ray data on one crystal of each complex were collected by FAST (Arndt, 1985) to 2.0 Å using the MADNES software (Messerschmidt & Pflugrath, 1987). Crystal orientation was refined prior to and during data collection, allowing reflections to be integrated and LP-corrected online. Data collection details are given in Table I. Merging of equivalents was performed with the Fox and Holmes (1966) algorithm by dividing the data into 5° batches on the scan angle (Ω), analogous to separate films. The resulting F_{PI}'s were combined with F_c's derived from endothiapepsin coordinates in the nonisomorphous cell. Sim–Luzatti weighted coefficients $2mF_o - 2DF_c$ (Read, 1986) were prepared by the program SIMWT (Tickle, 1988), which performs the derivative to native scaling. Difference Fouriers were calculated by FFT (Ten-Eyck, 1975) and displayed using FRODO (Jones, 1978) on an Evans and Sutherland PS390 raster graphics terminal. The initial maps allowed most of each inhibitor structure to be built prior to least-squares refinement, which was performed with RESTRAIN (Haneef et al., 1985) on the University of London CRAY-XMP supercomputer. Each inhibitor complex was subjected to several rounds of rebuilding and restrained refinement. Refinement results are given in Table II. The geometrical restraints used by FRODO and RESTRAIN were extended for the nonstandard residues of the inhibitors, e.g., cyclohexylstatine.

Molecular Modeling. The structures of PD125967 and PD125754 were extracted from the coordinate data for the complexes and transferred to a model of human renin (Sibanda et al., 1984) to evaluate steric compatibility, subsite occupation, and electrostatic interactions. Hydrogen bonds were identified by measuring the distance between the "heavy" atoms (X) involved and also the X–H···X angle for which a lower limit of 90° was used. Unfavorable steric contacts between inhibitor and enzyme were determined on the basis of "heavy" atom van der Waals radii reduced to 90%. A preliminary resolution of these contacts was sought by rotation of the enzyme side chains involved in the interactions.

RESULTS AND DISCUSSION

Inhibitor Conformation. The initial difference Fourier maps at 2.0 Å were of high quality (Figure 2) and allowed both inhibitors to be modeled from P_4 to P_2'. The electron density resulting from the refinement of both inhibitors is shown in Figure 3. All residues are clearly defined except the (dimethylamino)benzene group at P_3' of PD125754, which is probably disordered in solvent.

Both inhibitors adopt similar extended conformations with main-chain ϕ and ψ angles occupying the β-sheet region of

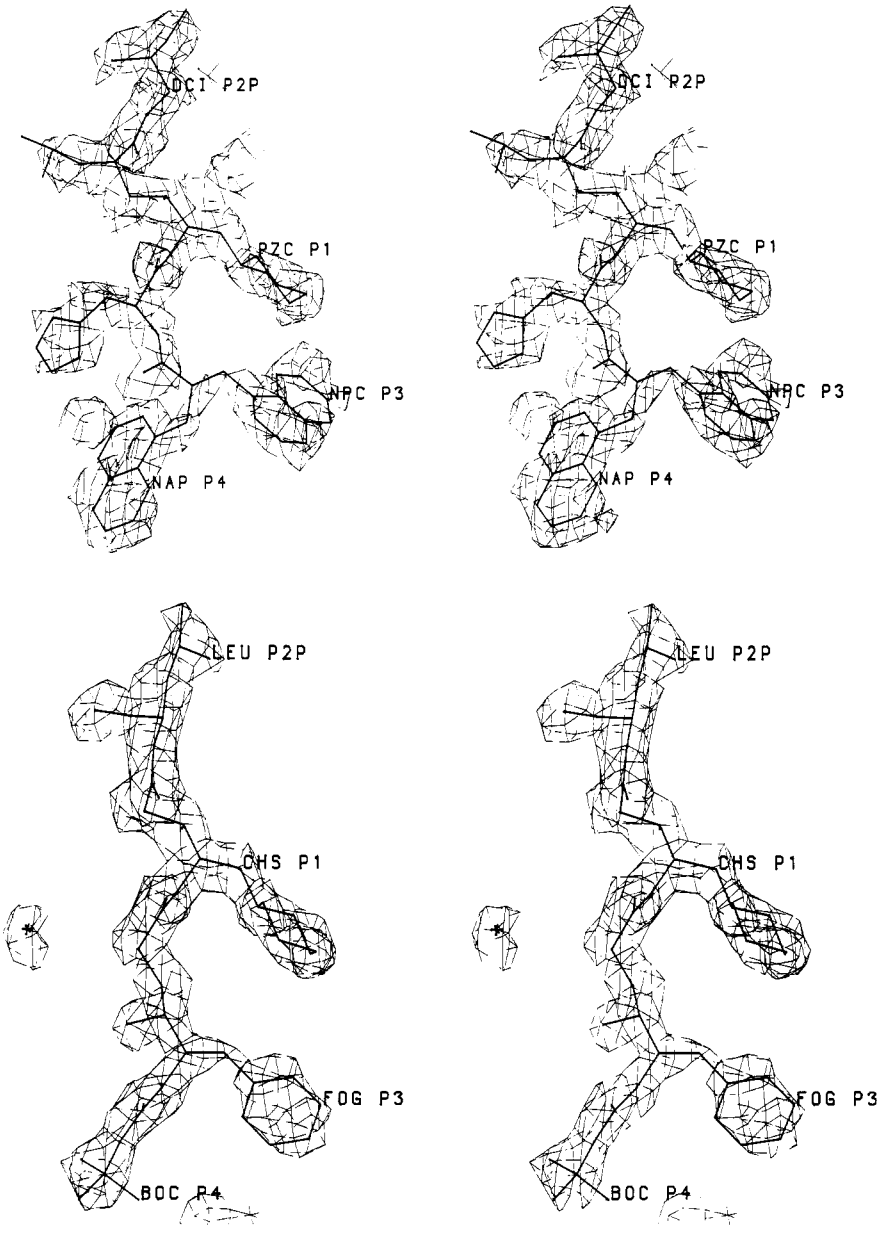

FIGURE 3: $2F_o - F_c$ electron density in stereo for PD125967 (top) and PD125754 (bottom). The electron density is shown in thin lines; inhibitors are shown in thick lines. P2P indicates the P_2' position.

the Ramachandran plot. Details of the interactions between enzyme and both inhibitors are shown in Figure 4. The residues at P_4–P_1 form an antiparallel β-sheet with residues 217–219. The central residues of each inhibitor (P_2–P_2') are shielded from solvent by the active site "flap" which also shields the catalytic center, consisting of the essential aspartates 32 and 215, from bulk solvent. The carboxyls of both aspartates are within hydrogen-bonding distance of the hydroxyl on the transition-state analogue at P_1. This, as with previous analyses, e.g., Foundling et al. (1987), suggests that the mode of binding of the inhibitors mimics productive binding of a substrate. In the case of PD125967 the P_1 isostere is a hydroxyethylene analogue whereas PD125754 possesses a cyclohexylstatine residue.

Least-squares fitting of the two inhibitor complexes using XS5 (A. Šali, unpublished work) to superimpose the enzyme moieties results in an rms deviation of 0.14 Å for all 330 residues. The inhibitors superimpose very closely from P_3 to P_1 despite large differences in main-chain and side-chain chemistry. Greater differences are seen in the P_1' region where statine lacks both a side-chain and one main-chain atom relative to a dipeptide.

The bis(1-naphthylmethyl)acetyl residue at P_3 of PD125967 resides in both the S_4 and S_3 pockets. This region of the renin active site cleft has a high proportion of hydrophobic residues (see Table III) (Sibanda et al., 1984). Accordingly, inhibition studies of renin have shown a preference for bulky hydrophobic residues at P_4 and P_3 [e.g., Luly et al. (1988)].

At P_4 the naphthyl group of PD125967 makes 22 van der Waals contacts (shorter than 4.0 Å) in contrast to the 11 contacts made by the smaller *tert*-butyloxycarbonyl of PD125754. The latter almost forms a seven-membered planar group arising from delocalization of electrons over the amide group and steric effects of the oxygen lone pairs. This oxygen appears to accept a hydrogen bond from a tightly bound water molecule (W1) (Figure 5). W1 is also within hydrogen-bonding distance of P_3 NH, P_3 OH, and Tyr 222 OH.

It was observed for endothiapepsin complexes that the presence of a cyclohexylmethyl group at P_1 of inhibitors induces

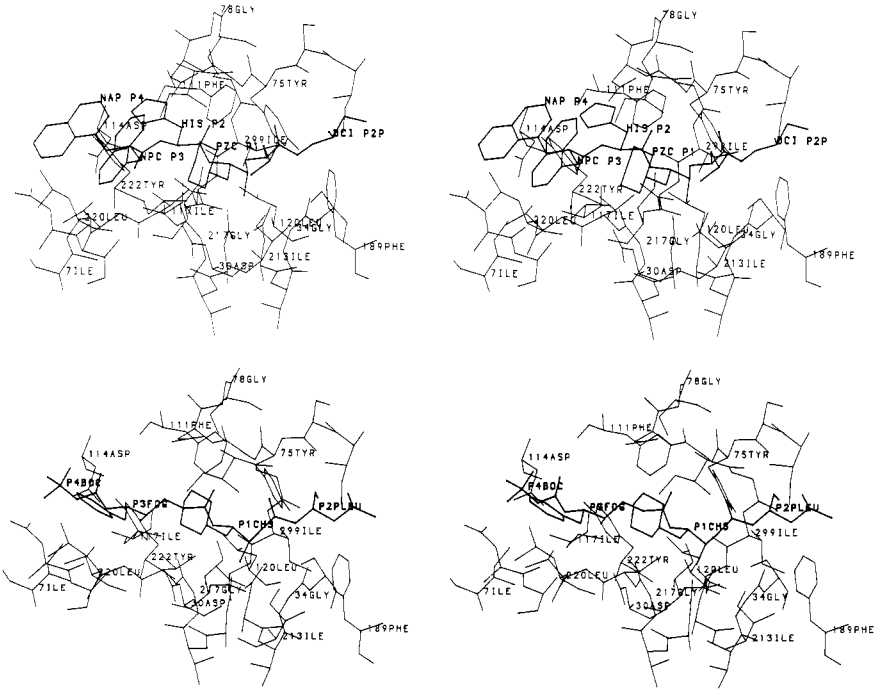

FIGURE 4: Refined structures of PD125967 (top) and PD125754 (bottom) in the context of the endothiapepsin active site. The inhibitors are shown in thick lines; enzyme residues are shown in thin lines.

Table III: Enzyme Residues in van der Waals Contact with One or Both Inhibitors at P_4 to P_2'[a]

position	all residues closer than 4.0 Å
P_4	Asp 12, Thr 219, Leu 220, Tyr 222, W1, W20
P_3	Ile 7, Asp 12, Ala 13, Asp 77, Ser 110, Asp 114, Gly 217, Thr 218, Thr 219, W1, W4
P_2	Tyr 75, Gly 76, Asp 77, Gly 217, Thr 218, Tyr 222, Ile 297, W1
P_1	Asp 30, Asp 32, Gly 34, Tyr 75, Gly 76, Asp 77, Phe 111, Leu 120, Asp 215, Gly 217, Thr 218, W4
P_1'	Gly 34, Tyr 75, Gly 76, Phe 189, Ile 213, Asp 215, Ile 299, Ile 301
P_2'	Gly 34, Ser 35, Ile 73, Ser 74, Tyr 75, Gly 76, Leu 128, Phe 189, W8

[a] Waters which interact with both are also shown (prefixed W).

a change in the bound conformation of the phenyl ring at P_3, causing it to adopt a sterically less favorable rotamer about χ_2 (Šali et al., 1989). This effect may account for the poorer potency of cyclohexylstatine analogues with endothiapepsin compared to inhibitors with a leucyl analogue at P_1 (Cooper et al., 1989). The P_3 naphthyl of PD125967 adopts a conformation consistent with other structures which have a cyclohexylmethyl filling S_1 [e.g., Šali et al. (1989)]. The steric bulk of the cyclohexyl at P_1 forces the naphthyl ring at P_3 to lie with its longest direction approximately perpendicular to the active site cleft. As a consequence, significant conformational changes occur in the side chains of two residues, namely, Asp 77 and Asp 114, which reside in the active site flap and a short stretch of α-helix (h_{N2}), respectively. These changes are shown in Figure 6 where the bound structures of both inhibitors are shown superimposed. We suggest that the favorable effect of the cyclohexyl group on potency for renin is due to the different size and shape of the contiguous S_1 and S_3 binding regions in this enzyme. This may allow bulky cyclohexyl and phenylalanyl side chains to be accommodated with less conformational change in the enzyme (or ligand).

The phenyl ring at P_3 of PD125754 might be expected to adopt the same orientation as found in other inhibitor complexes possessing Phe at P_3 and cyclohexylmethyl at P_1. For this inhibitor it is clear that the bulky cyclohexyl group at P_1 does not induce a large rotation around χ_2 of the P_3 Phe as occurs in previously studied compounds of this type (see above). We suggest that this is due to a subtle effect of the hydroxyethylene analogue joining the P_3 and P_2 residues. This is free from the planar restraints of an ordinary peptide bond, and rotation of the dihedral angles would allow unfavorable interactions between the aromatic and cyclohexyl rings to be relieved without a dramatic change in χ_2 of the phenyl residue.

P_3 residues usually form two main-chain hydrogen bonds with Thr 219. In the case of PD125967, where the NH of P_3 is replaced by a methylene group, only one such interaction occurs in which the P_3 carbonyl accepts a hydrogen bond from NH Thr 219. The other generally conserved interaction involving NH P_3 and OH Thr 219 is formed in the PD125754 complex. This inhibitor has an *S*-hydroxyl group in place of the P_3 carbonyl. However, the hydrogen bonds involving NH Thr 219 as well as a tightly bound water molecule (W1) are formed. Hence, replacement of a peptide group, which would otherwise render the inhibitor susceptible to chymotrypsinolysis, with the hydroxyethylene analogue allows conserved hydrogen bonds to be retained. The hydrogen bonds at P_3 may be important for tight binding of substrates since, for any series of synthetic peptides, a large increase in k_{cat}/K_m is observed for those which occupy S_3 (Fruton, 1976, 1987). The consistency of the kinetic and structural data for the P_3 position serves to reinforce our belief that the mode of binding observed with the inhibitors is a productive one.

In general, the greatest diversity of side-chain conformation is found at P_2 where histidine side chains can adopt conformations separated by about 120° on χ_2 (Foundling et al., 1987). A conformation involving van de Waals interactions with Asp 77 and Tyr 222 is adopted in PD125967. This was

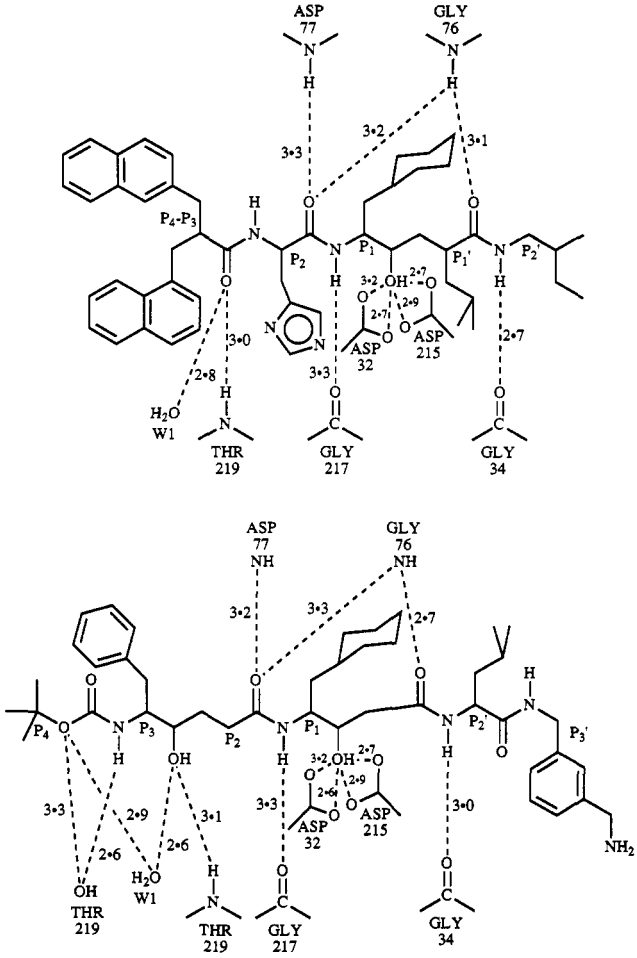

FIGURE 5: Schematic diagrams showing the hydrogen bonds formed by each inhibitor molecule with the enzyme (PD125967, top; PD125754, bottom). Bound waters are prefixed W. The donor–acceptor atom distances are shown in angstroms.

found for other inhibitors, e.g., the reduced bond analogue H-142 (Foundling et al., 1987). An alternative conformation occurs with inhibitors containing the dipeptide analogue statine which lacks a P_1' side chain. The same applies to hydroxyethylene analogues with small side chains at P_1', e.g., Leu$\underline{\text{OH}}$Val, where the imidazole ring at P_2 has been found occupy the otherwise partly empty S_1' pocket. In PD125967 it appears that the P_2 imidazole is excluded from the S_1' pocket by the bulk of the P_1' leucine side chain. In contrast, for PD125754 the S_2 and S_1' pockets are not filled due to the absence of inhibitor side chains at these positions although one water molecule (W323) occupies the S_2 subsite and another (W322) residues in the S_1' region. Neither of these water sites occur in the PD125967 complex. The carbonyls at P_2 of both PD125967 and PD125754 are involved in conserved bifurcated hydrogen bonds to the peptide nitrogens of flap residues Gly 76 and Asp 77. In endothiapepsin complexes the amide nitrogen at P_2 is often not hydrogen bonded to the enzyme, as is found for PD125967. This suggests that replacement of the P_2 peptide nitrogen with the nonpolar methylene group of PD125754 may not have deleterious consequences for the affinity.

The cyclohexylmethyl moieties at P_1 of both inhibitors are involved in 21 van der Waals contacts (≤4.0 Å) with the enzyme which forms a predominantly hydrophobic pocket involving the side chains of Tyr 75, Phe 111, and Leu 120. However, two polar residues, namely, aspartates 30 and 77, also make several side-chain interactions. The P_1 main chains form conserved hydrogen bonds between their peptide amines and the carbonyl of Gly 217. More importantly, the P_1 hydroxyl oxygen of both isosteres is within hydrogen-bonding distance of all four carboxyl oxygens of the catalytic aspartates. Possible locations of the P_1 hydroxyl hydrogen were explored by rotation of the >CH–OH dihedral angle with a model hydrogen atom attached to the oxygen having idealized sp^3 hybridization. Two possible positions were found for the hydrogen, assuming that it lies in the plane of the essential carboxyls. In one position it would interact with the outer O^δ of Asp 215, and in the other it would interact with the inner O^δ of Asp 32, suggesting that one of these oxygens carries the negative charge and the other a proton which could interact with one lone pair on the hydroxyl oxygen. Accordingly, these are the shortest of the four OH to O^δ distances in both complexes (≈2.6 Å) (Figure 5). For the OH hydrogen to interact with the outer O^δ of Asp 215, the O–H bond would be eclipsed with the CHOH–CH_2 bond of the isostere, whereas the alternative interaction with Asp 32 involves a staggered and hence more favorable conformation about the CH–OH bond. The electron density for the inner O^δ Asp 32 and OH P_1 is contiguous, and although this may be due to the resolution limit (2.0 Å), it suggests that the OH hydrogen may preferentially reside between these atoms. This suggests that the outer oxygen of Asp 215 may possess the proton since this oxygen forms the second shortest contact with the hydroxyl oxygen. However, there are no good reasons why a number of other arrangements should not exist in static or dynamic equilibrium such as that suggested by Suguna et al. (1987), in which the outer oxygen of Asp 215 possesses the negative charge.

The S_1' side-chain pocket is left empty by PD125754, in which the statine residue spans both S_1 and S_1' pockets although the latter is partly occupied by a bound water molecule (W322). The carbonyl oxygen of the statine residue accepts a hydrogen bond from the NH of Gly 76. The same interaction is made by the P_1' carbonyl of PD125967, confirming that statine behaves as a dipeptide analogue (Cooper et al., 1989). The leucine side chain at P_1' of PD125967 interacts with several hydrophobic residues of the C-terminal domain, namely, Phe 189, Ile 213, Ile 299, and Ile 301, which form a patch contiguous with S_2.

The P_2' side chains of both inhibitors (Ile in PD125967 and Leu in PD125754) lie in very similar positions, making contacts with Ile 73, Leu 128, and Phe 189. The P_2' peptide amines of both inhibitors donate hydrogen bonds to the carbonyl of Gly 34. Unfortunately, electron density for the (dimethylamino)benzene moiety of PD125754 was not found, indicating that this residue is disordered in the solvent of the crystal, probably contributing little to the binding energy for endothiapepsin.

Relative Affinity. As can be seen in Table IV, PD125967 has a 2 order of magnitude stronger potency for endothiapepsin than PD125754, the latter being a relatively weak inhibitor. In contrast, both inhibitors are almost equipotent against renin, with PD125754 exhibiting slightly tighter binding. A rationale for the behavior of these molecules with endothiapepsin is provided by examination of the cocrystal structures reported here. The harder task of understanding the potencies of these compounds for renin has been tackled by docking the experimentally derived inhibitor structures into a model of human renin based on the endothiapepsin coordinates (Sibanda et al., 1984), as described later.

From inspection of Figure 5 it is clear that PD125754 makes three more hydrogen bonds to endothiapepsin than PD125967 since the latter possesses apolar functionalities at P_4–P_3. The

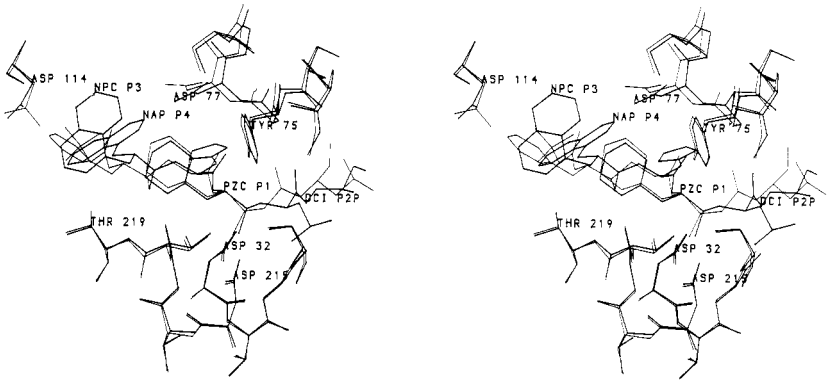

FIGURE 6: Superposition of the bound structures of PD125967 (thick lines) and PD125754 (thin lines) shown in stereo. Active site cleft residues 32–35, 215–219, 73–79, and 114 are shown for comparison. The very bulky naphthyl group at P_3 of PD125967 induces small conformational changes in Asp 77 and Asp 114 (top left).

Table IV: Inhibitory Potencies of PD125967 and PD125754 for Endothiapepsin and Renin

compound	endothiapepsin K_i (nM)	renin IC_{50} (nM)
PD125967	242 ± 97	170
PD125754	16180 ± 4077	22

Table V: Number of van der Waals Interactions ($d \leq 4.0$ Å) for Each Residue of the Inhibitors[a]

position	PD125967	PD125754
P_4	22 (naphthyl)	11 (Boc)
P_3	37 (naphthyl)	25 (Phe)
P_2	22 (His)	10 (Gly)
P_1	39 (cyclohexyl)	42 (cyclohexyl)
P_1'	20 (Leu)	14 (Gly)
P_2'	13 (Ile)	19 (Leu)
total	153	121

[a] Side-chain types are shown in parentheses.

hydrogen bonds involving the NH of P_3 and the *tert*-butyloxy group at P_4 of PD125754 cannot be formed in the PD125967 complex which possesses a bis(1-naphthylmethyl)alanine at these positions. However, hydrogen bonds are thought to be less important than other effects for determining the relative affinities of ligands. This is because although there is a favorable enthalpy change on forming NH → OC bonds from H_2O ← HN and CO ← HOH in solution, the contribution to ΔG is relatively small (Ptitsyn, 1973). Therefore, the number of van der Waals and charge–charge interactions as well as the hydrophobic and entropic effects of displacing bound water molecules from both inhibitor and enzyme into the more disordered solvent lattice must dominate. From Table V it can be seen that PD125967 makes significantly more van der Waals interactions with the enzyme than PD125794 at positions P_4, P_3, P_2, and P_1'. In addition, it appears that the histidine side chain of PD125967 may be involved in a charge–charge interaction with Asp 77.

Calculation of the solvent-accessible contact areas for free inhibitor, free enzyme, and the complex using a probe radius of 1.4 Å (Richmond & Richards, 1978) shows that PD125967 binding causes a loss of about 480 Å^3 for both enzyme and inhibitor whereas PD125754 causes a much smaller reduction in solvent-accessible area of 370 Å^3. Most of this difference can be attributed to the greater bulk of the side chains at P_4, P_3, P_2, and P_1' of PD125967 which are either smaller or absent in PD125754. The absence of side chains at P_2 and P_1' of this inhibitor results in significantly fewer interactions with the carboxy-terminal domain of endothiapepsin. Hence, the indications are that PD125967 will bind more strongly to endothiapepsin than PD125754. This prediction is clearly borne out by the K_i data (Table IV), which show that PD125967 has a 2–3 order of magnitude greater affinity than PD125754.

Modeling Interactions in Renin. Table IV shows the affinities for PD125967 and PD125754 for human renin. In contrast to the endothiapepsin data, the relative affinities of these compounds for renin are reversed and far more equivalent. The inhibitor structures from the endothiapepsin complexes were docked into a model of renin (Sibanda et al., 1984) in an effort to interpret these results (Figure 7).

The hydrogen bonds observed between the endothiapepsin-bound structure of PD125967 and the renin cleft are listed in Table VI. Most of the endothiapepsin hydrogen bonds are conserved in the renin model with the exception of that between P_2 CO and 76 NH. In renin Gly 76 is replaced by serine, which would alter the flap conformation. The P_4 naphthyl group in PD125967 is sterically compatible with the S_4 pocket of renin and forms a favorable edge-on interaction with Tyr 220. Conversely, the naphthyl group at P_3 has a close contact with Thr 12 and Gln 13, contacts with the latter residue being most severe. In endothiapepsin Gln 13 is replaced by alanine, leading to a larger S_3 pocket with no unfavorable interactions with the naphthyl ring. Similarly, at the S_2 subsite, the inhibitor histidine side chain makes an unfavorable steric interaction with Ser 76 of the flap which is not removed by rotation of the serine side chain. In endothiapepsin, the equivalent residue (Gly 76) provides a much larger pocket for ligand occupation. At both the S_3 and S_2 pockets these steric interactions may only be relieved by conformational changes in the inhibitor or enzyme. At S_1, the cyclohexyl group has a close contact with Phe 112 that can be removed by rotating the Phe side chain. Residue 30 at the S_1 pocket is aspartate in endothiapepsin but valine in renin, resulting in a more lipophilic environment for the cyclohexyl side chain of the inhibitor. The P_1' leucine of PD125967 makes an unfavorable contact with Ser 76 although this can be relieved by rotation of the serine side chain. The P_2' isoleucine collides with Leu 73 and Gln 128 (Ile and Leu in endothiapepsin, respectively). These contacts may also necessitate a conformational change in the inhibitor or enzyme, relative to the endothiapepsin-bound structure.

Hydrogen bond interactions made by PD125754 with the renin model are shown in Table VI. The replacement of Leu 220 in endothiapepsin with Tyr in renin results in a steric contact with the P_4 Boc group which can be resolved by slight rotation of the alkoxy group. At P_3 contacts with Thr 12 and especially Gln 13 may force the phenyl side chain to adopt a

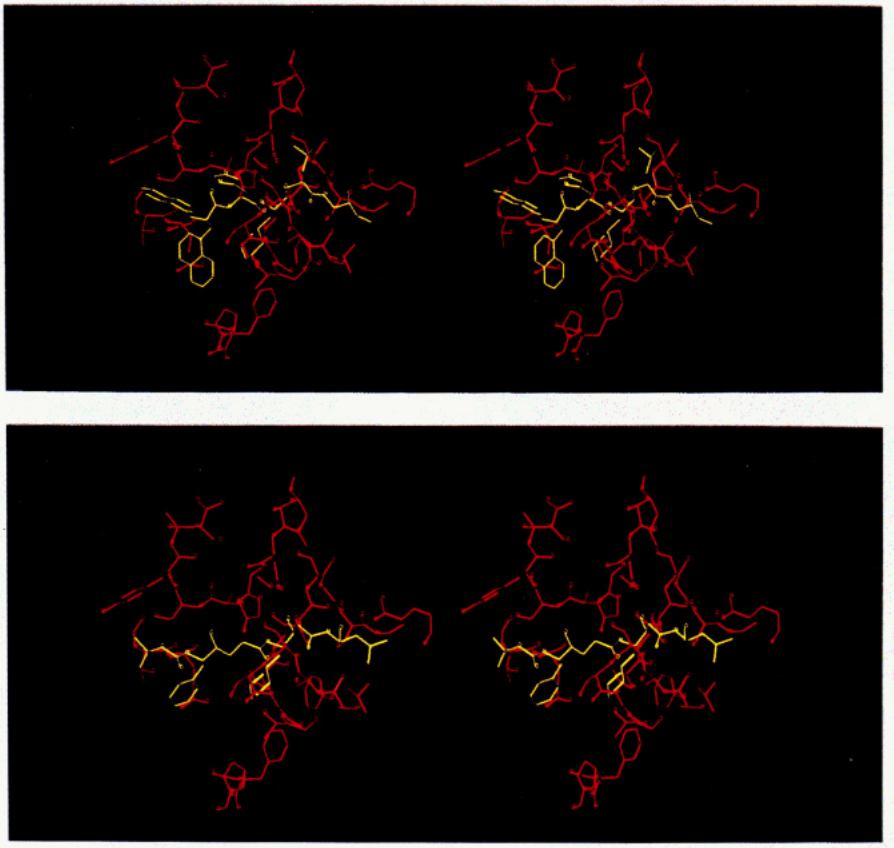

FIGURE 7: Models of PD125967 (top) and PD125754 (bottom) docked with the model of human renin. The inhibitors are shown in yellow with the model of the enzyme in red. The inhibitors are oriented with P_4 on the left and P_2' to the right.

Table VI: Hydrogen Bond Interactions between the Inhibitors and the Human Renin Model

PD125967	enzyme	PD125754	enzyme
P_3 CO	NH Ser 219	P_4 O	OH Ser 219[a]
P_2 CO	NH Thr 77	P_3 NH	OH Ser 219[a]
P_1 NH	CO Gly 217	P_3 OH	NH Ser 219
P_1 OH	COO Asp's 32 and 215	P_2 CO	NH Thr 77
		P_1 NH	CO Gly 217
P_1' CO	NH Ser 76	P_1 OH	COO Asp's 32 and 215
P_2' NH	CO Gly 34		
		P_1' CO	NH Ser 76
		P_2' NH	CO Gly 34

[a] Indicates hydrogen bond which could be formed by side-chain rotation.

different conformation from that found in endothiapepsin. The S_2 and S_1' subsites are not occupied by this inhibitor, which has the equivalent of a glycine at these positions. As with PD125967 there is a close contact between the P_1 cyclohexyl group and the phenyl ring of 112 which can be resolved by small conformational changes. Close contacts between the alkyl group at P_2' and enzyme residues Gln 128 and Leu 73 probably indicate the need for conformational changes in the inhibitor.

In summary, the modeling studies show that the main-chain conformations of these novel inhibitor structures are transposable from endothiapepsin to renin without large changes in dihedral angles. Nearly all hydrogen bonds to the inhibitors are conserved in both enzymes. The orientations of the side chains at P_4, P_1, and P_1' of the endothiapepsin complexes could be considered close approximations to the renin-bound conformations. In contrast, the unfavorable interactions at S_3, S_2, and S_2' indicate that renin or the inhibitor will deviate most from the endothiapepsin-bound conformation at these positions. These subsites are where the active site cleft of renin has a number of critical amino acid replacements affecting the composition and size of the pockets. The differences between endothiapepsin and renin at these pockets are presumably responsible for the different kinetic behavior of each enzyme with the two inhibitors. Moreover, the structural and modeling studies presented here suggest that the extra bulk of certain PD125967 side chains, especially P_3, may weaken its binding to renin relative to PD125754 for steric reasons.

ACKNOWLEDGMENT

We thank our colleagues C. Dealwis, V. Dhanaraj, D. Bailey, A. Beveridge, S. Wood, M. Badasso, C. Aguilar, J. Pitts, M. Crawford, M. Newman, and I. J. Tickle for many useful discussions.

REFERENCES

Arndt, U. W. (1985) *Methods Enzymol. 114*, 472–485.

Blundell, T. L., Jenkins, J., Pearl, L., Sewell, T., & Pederson, V. (1985) in *Aspartic Proteinases and their Inhibitors* (Kostka, V., Ed.) pp 151–161, Walter de Gruyter, Berlin.

Blundell, T. L., Cooper, J. B., Foundling, S. I., Jones, D. M., Atrash, B., & Szelke, M. (1987) *Biochemistry 26*, 5585–5590.

Boger, J., Payne, L. S., Perlow, D. S., Lohr, N. S., Poe, M., Blaine, E. H., Ulm, E. H., Schorn, T. W., Lamont, B. I., Lin, T.-Y., Kawai, M., Rich, D. H., & Veber, D. F. (1985) *J. Med. Chem. 28*, 1779–1790.

Bolis, G., Fung, A. K. L., Greer, J., Kleinert, H. D., Marcotte, P. A., Perun, T. J., Plattner, J. J., & Stein, H. H. (1987) *J. Med. Chem. 30*, 1729–1737.

Cooper, J. B. (1989) Ph.D. Thesis, University of London.

Cooper, J. B., & Harris, C. J. (1988) *Curr. Cardiovas. Pat. 1*, 143–157.

Cooper, J. B., Foundling, S. I., Blundell, T. L., Boger, J., Jupp, R. A., & Kay, J. (1989) *Biochemistry 28*, 8596–8603.
Dunn, B. M., Jimenez, M., Parten, B. F., Valler, M. J., Rolph, C. E., & Kay, J. (1986) *Biochem. J. 237*, 899–906.
Foundling, S. I., Cooper, J., Watson, F. E., Cleasby, A., Pearl, L. H., Sibanda, B. L., Hemmings, A., Wood, S. P., Blundell, T. L., Valler, M. J., Norey, C. G., Kay, J., Boger, J., Dunn, B. M., Leckie, B. J., Jones, D. M., Atrash, B., Hallett, A., & Szelke, M. (1987) *Nature (London) 327*, 349–352.
Fox, G. C., & Holmes, K. C. (1966) *Acta Crystallogr. 20*, 886–891.
Fruton, J. S. (1976) *Adv. Enzymol. Relat. Areas Mol. Biol. 44*, 1–36.
Fruton, J. S. (1987) in *Hydrolytic enzymes* (Neuberger, A., & Brocklehurst, K., Eds.) pp 1–37, Elsevier Science Publishers, Amsterdam.
Haneef, I., Moss, D. S., Stanford, M. J., & Borkakoti, N. (1985) *Acta Crystallogr. A41*, 426–433.
Hudspeth, J. P., Kaltenbronn, J. S., Repine, J. T., & Woo, P. W. K. (1989) U.S. Patent No. 4,863,905, Sept 5, 1989.
Iizuka, K., Kamijo, T., Kubota, T., Akahane, K., Umeyama, H., & Kiso, Y. (1988) *J. Med. Chem. 31*, 701–704.
Jones, T. A. (1978) *J. Appl. Crystallogr. 11*, 268–272.
Kaltenbronn, J. S., Hudspeth, J. P., Lunney, E. A., Michniewicz, B. M., Nicolaides, E. D., Repine, J. T., Roark, W. H., Stier, M. A., Tinney, F. J., Woo, P. K. W., & Essenburg, A. D. (1990a) *J. Med. Chem. 33*, 838–845.
Kaltenbronn, J. S., Hudspeth, J. P., Lunney, E. A., Nicolaides, J. T., Repine, J. T., Roark, W. H., Stier, M. A., Tinney, F. J., Woo, P. K. W., & Essenburg, A. D. (1990b) in *Peptides, Chemistry, Structure and Biology* (Rivier, J. E., & Marshall, G. R., Eds.) Proceedings of the Eleventh American Peptide Symposium, pp 404–405, Escom, Leiden.
Kissei (1988) U.S. Patent, Patent No. 4,656,269, Jan 13, 1988.
Kokubu, T., Hiwada, K., Murakami, E., Imamura, Y., Matsueda, R., Yabe, Y., Koike, H., & Iijima, Y. (1985) *Hypertension 7* (Suppl. I), 8–11.
Kokubu, T., Hiwada, K., Nagae, A., Murakami, E., Morisawa, Y., Yabe, Y., Koike, H., & Iijima, Y. (1986) *Hypertension 8* (Suppl. II), 1–5.
Leckie, B. J. (1985) in *Aspartic Proteinases and their Inhibitors* (Kostka, V., Ed.) pp 443–461, Walter de Gruyter, Berlin.
Luly, J. R., Yi, N., Soderquist, J., Stein, H., Cohen, J., Perun, T. J., & Plattner, J. J. (1987) *J. Med. Chem. 30*, 1609–1616.
Luly, J. R., BaMung, N., Soderquist, J., Fung, A. K. L., Stein, H., Kleinert, H. D., Marcotte, P. A., Egan, D. A., Bopp, B., Merits, I., Bolis, G., Greer, J., Perun, T. J., & Plattner, J. J. (1988) *J. Med. Chem. 31*, 2264–2276.
Messerschmidt, A., & Pflugrath, J. W. (1987) *J. Appl. Crystallogr. 20*, 306–315.
Moews, P. C., & Bunn, C. W. (1970) *J. Mol. Biol. 54*, 395–397.
Ptitsyn, O. B. (1973) *Pure Appl. Chem. 31*, 227–244.
Read, R. J. (1986) *Acta Crystallogr. A42*, 140–149.
Richmond, T. J., & Richards, F. M. (1978) *J. Mol. Biol. 119*, 537–555.
Rosenberg, S. H., Plattner, J. J., Woods, K. W., Stein, H. H., Marcotte, P. A., Cohen, J., & Perun, T. J. (1987) *J. Med. Chem. 30*, 1224–1228.
Šali, A., Veerapandian, B., Cooper, J. B., Foundling, S. I., Hoover, D. J., & Blundell, T. L. (1989) *EMBO J. 8*, 2179–2188.
Sibanda, B. L., Blundell, T. L., Hobart, P. M., Fogliano, M., Bindra, J. S., Dominy, B. W., & Chirgwin, J. M. (1984) *FEBS Lett. 174*, 102–111.
Suguna, K., Padlan, E. A., Smith, C. W., Carson, W. D., & Davies, D. R. (1987) *Proc. Natl. Acad. Sci. U.S.A. 84*, 7009–7013.
Szelke, M. (1985) in *Aspartic Proteinases and their Inhibitors* (Kostka, V., Ed.) pp 421–441, Walter de Gruyter, Berlin.
Szelke, M., Leckie, B., Hallett, A., Jones, D. M., Sueiras-Diaz, J., Atrash, B., & Lever, A. F. (1982) *Nature 299*, 555–557.
Ten Eyck, L. F. (1973) *Acta Crystallogr. A29*, 183–191.
Tickle, I. J. (1988) in *Improving Protein Phases* (Bailey, S., Dodson, E., & Phillips, S. Eds.) pp 130–137, SERC, Daresbury Laboratory, U.K.